Int J Clin Exp Med 2020;13(10):7406-7414
www.ijcem.com /ISSN:1940-5901/IJCEM0111504

Original Article

SCG10 protein maintenance in superior cervical ganglia promotes sympathetic hyperinnervation after myocardial infarction

Junyi Zhang[1,2], Kaidi Zhao[2], Yan Li[1,3], Yugen Shi[1,3], Wenju Yan[1], Qian Liu[1], Suhua Yan[1,3]

[1]Department of Cardiology, Shandong Qianfoshan Hospital, Cheeloo College of Medicine, Shandong University, Shandong, China; [2]Department of Cardiology, Qingdao Municipal Hospital, Qingdao, Shandong, China; [3]Department of Cardiology, Shandong Provincial Qianfoshan Hospital, The First Hospital Affiliated to Shandong First Medical University, Shandong, China

Received March 27, 2020; Accepted May 28, 2020; Epub October 15, 2020; Published October 30, 2020

Abstract: Objective: Our research aimed to investigate whether superior cervical ganglia (SCG) neuron expressing SCG10, and whether SCG10 is involved in sympathetic nerve remodeling after MI. Methods: Adult male Sprague-Dawley rats were divided into a control group, MI group, and MI+SCG10 degeneration inhibitor group. Western blotting and immunoflurescent staining were used to detect SCG10 expression level and location in this study. The time course of SCG10 level variances of SCG and cardiac tissue were obtained by protein analysis on day 0, 1, 3 and 7 using western blotting. Results: From the third day of myocardial infarction, we found that the number of SCG10 cells increased significantly, not only the number of positive cells, but also more expression in the cytoplasm, and there was a significant difference compared with the sham group ($P < 0.01$). SCG10 positive cells of the MI7D group increased significantly compared with the MI3D group ($P < 0.01$). The content of SCG10 in MI7D group was significantly lower than that in MI7D+SP600125 group in the SCG ($P < 0.01$). The expression of TH in MI7D group was significantly higher than that in the sham group ($P < 0.01$). The content of TH in MI7D group was significantly lower than that in MI7D+SP600125 group ($P < 0.01$). The SCG10 level in the MI3D was significantly higher than that in the sham group ($P < 0.01$). MI7D group increased significantly compared with the MI3D group ($P < 0.01$). The content of SCG10 in MI7D group was significantly lower than that in MI7D+SP600125 group in the SCG ($P < 0.01$). Conclusion: SCG10 overexpression in sympathetic neurons of SCG might lead to cardiac sympathetic nerve hyperinnervation, and SCG10 could be a new target for regulating cardiac sympathetic activity after MI.

Keywords: Superior cervical ganglion-10, superior cervical ganglion, myocardial infarction, sympathetic hyperinnervation

Introduction

Malignant arrhythmia after myocardial infarction (MI) is an important cause of death and disability. Many previous studies have shown that excessive hyperplasia and imbalance of sympathetic nerve distribution after MI are the most important factors in the pathogenesis of malignant arrhythmia [1]. Research on the mechanism of sympathetic hyperproliferation has attracted much attention at present. Recent studies have focused on γ-aminobutyric acid (GABA) signaling system and inflammation pathway in sympathetic nerve remodeling and susceptibility to malignant arrhythmias after MI [2, 3]. Relevant conclusions have been drawn, but the mechanism is still unclear.

Superior cervical ganglion-10 (SCG10), also known as stathmin 2 (STMN2), a neuron-specific member of the stathmin family of proteins, is an important marker of regenerating sensory axons [4]. It has been reported that SCG10 can not only be used as a marker of nerve injury, but also can affect the survival time of the severed distal nerve [5]. In addition, some investigators have found that the levels of SCG10 are increased in the end bulbs of the proximal stump in both the central and peripheral nervous systems [6]. Furthermore, the binding of

SCG10 to tubulin regulates the polymerization and depolymerization of microtubules, which is a key in axonal regeneration [7].

Clinical research demonstrates that removal of the superior cervical ganglion (SCG) results in the disappearance of symptoms of angina pectoris and the increase of blood pressure and cardiac sympathetic activity [8]. Our experimental group also confirmed that some signal systems in SCG regulates NE release in cardiac sympathetic nerves and intracellular Ca2+ levels after MI. Therefore, we envisage that after MI the level of SCG10 in the SCG may increase and promote the regeneration of sympathetic nerves around the infarct area [9]. To confirm the idea above, we made a rat model of MI to examine whether SCG10 increased in the SCG and the infarct periphery after the onset of MI. Further, rats were injected with SP600125 intraperitoneally three times a week, so as to observe whether the changes in SCG10 content are significantly correlated with the changes in the secretion of TH in the nerve endings.

Materials and methods

Animal and experimental protocol

Adult male Sprague-Dawley rats (220-250 g, Vital River, Beijing, China) were used. They were housed in cages (3-5 rats per cage) with wood shaving bedding and maintained in a temperature-controlled room (22se°C) with daily exposure to a twelve-hour light-dark cycle. All procedures were based on the ethical standards of animal research approved by Shandong University Institutional Animal Care and Use Committee. All efforts were made to minimize their suffering. Two separate experiments were conducted. Protocol 1: 40 rats were enrolled and randomly divided into four groups: the sham surgery group (sham group, n=8), 1 day of cardiac infarction group (MI1D group, n=18), 3 days of MI group (MI3D group, n=18), and 7 days of MI group (MI7D group, n=17). Protocol 2: 30 rats were enrolled and randomly divided into three groups: the sham surgery group (sham group, n=8), rats with MI for 7 days (MI7D group, n=17), and rats with MI for 7 days treated with JNK inhibitor SP600125 (Sigma) (MI7D+SP600125 group, n=18). JNK can phosphorylate some sites on the SCG10 domain, thus accelerating the decomposition of SCG10. SP600125 is a reversible and ATP-competitive JNK inhibitor, which can reduce the effect of JNK on SCG10 phosphorylation and slow down the degradation of SCG10. SP600125 was intraperitoneally injected at 5 mg/kg three times a week. The rats were sacrificed and the tissue was frozen at -80°C for further biochemical analysis or embedded in OCT for histological examination.

Experimental myocardial infarction

SD rats were anesthetized by an intra-peritoneal injection of 30 mg/kg of 3% sodium pentobarbital (Sigma-Aldrich, St. Louis, MO, USA). Then we placed the rats in a supine position on a homeothermic heating pad in order to maintain their body temperature. We shaved their fur from the neck and chest areas with an electric shaver. Endotracheal intubation was performed to maintain the breathing by making a 5 mm mid-neck incision and retraction of muscle tissue. The endotracheal tube was inserted into the trachea and connected to a small-animal respirator (HX-300S, TME, Chengdu, China) at 70 breaths/min and a tidal volume of 1.2 ml/100 g body weight. The chest was incised at the left fourth intercostal space, the tissue layers were divided, and a small incision was made in de pleura so that the heart was exposed. Then we ligated the area between the left atrial appendage and the pulmonary artery cone with a 6-0 prolene suture. The infarction was confirmed by ST segment elevation with electrocardiograph. Then we sutured the muscle and skin and removed the respirator. The rats were closely monitored and taken care of in the recovery period. At the end of surgery, they were injected with penicillin (800,000 U, NCPC).

Harvesting the superior cervical ganglion

The preparatory work was the same as that of the rat myocardial infarction model. After incision of the skin and soft tissue of the rat's neck, we saw the sternohyoid muscle with a median field of vision and the sternomastoideus muscle on both sides of the subdivision. After blunt separation of these two muscles, the common carotid artery was bent out of shape. After the superior thyroid artery and the common carotid artery were bifurcated, the oval superior cervical ganglion could be seen above the vagosympathetic chain. Once the rat's myocardial infarction was confirmed, removal of the *superior cervical ganglion* was carried out.

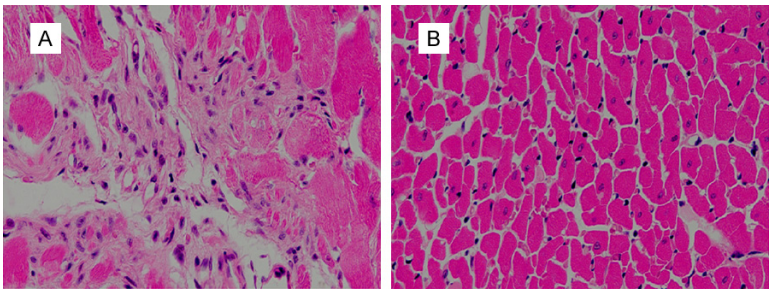

Figure 1. Myocardial histopathology of myocardial infarction rats and sham operated rats. A. Myocardial infarction rats, Vacuolar degeneration, partial rupture, unclear, disappearance and diffuse inflammatory cell infiltration can be seen in myocardial tissue. B. The normal myocardial tissue showed that the morphology of myocardial cells was complete and clearly defined, the striation in the cytoplasm was clear, and the nucleus was oval.

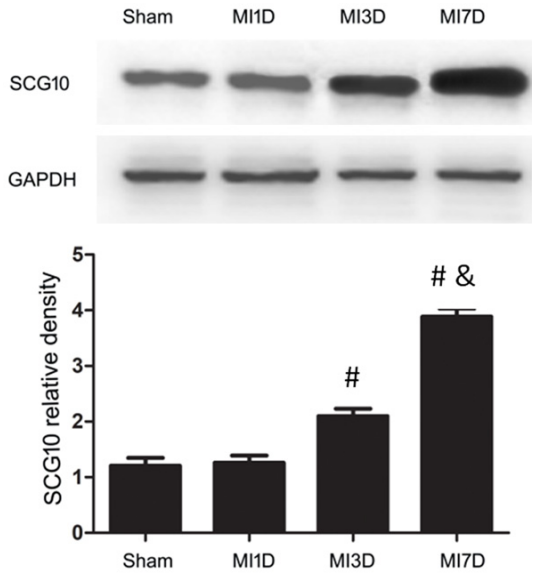

Figure 2. Western blot showing the expression profiles of SCG10 in the SCG after MI. SCG10 was quantified relative to the GAPDH (37 KD) levels. #P < 0.01 vs. sham; &P < 0.01 vs. MI3D.

Immunofluorescence

SCGs and hearts were immersed in 30% sucrose in PBS, embedded in OCT compound (Tissue-Tek), and frozen in a freezer whose temperature was kept at -80°C. For tissue processing, samples were incubated with primary antibodies anti-STMN2 (1:400; Proteintech) or anti-tydroxylase (1:200; Millipore) overnight at 4°C followed by a two-hour incubation with Alexa Fluor 546 donkey anti-rabbit (1:400; Peprotech) and FITC-conjugated rabbit anti-sheep (1:200; Bethyl) secondary antibodies. In order to identify the nuclei, we used DAPI (Life Technologies) counterstain in the sections. We used Image-Pro Plus 5.0 to calculate and measure the area of stained nerves divided by the total area examined ($\mu m^2/mm^2$). The selected fields are as we previously described.

Western blot analysis

We extracted proteins by using a Protein Extraction Kit (Beyotime Institute of Biotechnology, Jiangsu, China). Extracted proteins from different tissues were measured with the BCA Protein Assay Kit (Pierce). The same amount of protein from each sample underwent electrophoresis on a 12% SDS-PAGE gels and transferred to polyvinylidene difluoride (PVDF) membranes. The membranes were blocked in 5% non-fat dry milk in TBST (TBS containing 0.05% Tween-20) incubated overnight at 4% with primary rabbit anti-STMN2 (1:2000; Proteintech). Then membranes were probed with anti-rabbit secondary antibodies (1:5000; Zhong Shan-Golden Bridge Biotechnology) for 1 h. Enhanced chemiluminescence (ECL) detection kit (Millipore) was used to visualize the membrane. Visualization and quantification of the densities were performed using the FluorChem E Image (Protein-Simple, Santa Clara, CA, USA) and NIH Image software. Protein densities were analyzed relative to individual GAPDH densities.

Statistical analysis

Analyses were performed using SPSS 17.0 software (SPSS Inc. Chicago, IL, USA). All statistical analyses were considered significant at *P*-values < 0.05.

Results

Pathological morphology

Pathological H&E staining was performed in myocardial infarction rats and operation group rats. The results showed that there was vacuolar degeneration, partial rupture, unclear, disappeared and diffuse inflammatory cells infiltrating the infarct site. The normal myocardial tissue showed that the morphology of myocardial cells was complete and clearly defined, the striation in the cytoplasm was clear, and the nucleus was oval (**Figure 1**).

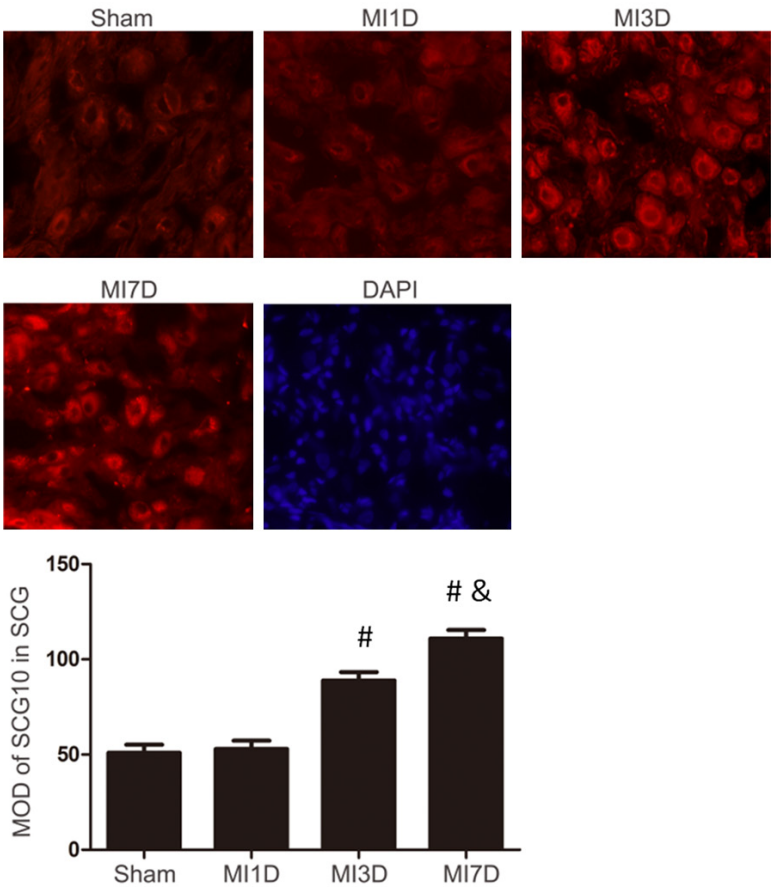

Figure 3. The immunofluorescence of SCG10 in SCG after myocardial infarction (MI). The positive cells presented red fluorescence. The image shows that SCG10 of the sham group mainly gather around the nucleus, but less in the cytoplasm. The MI1D group is similar to the sham group, and no significant change. The number of SCG10 increase significantly, not only the number of positive cells, but also more expression in the cytoplasm in the MI7D group. #P < 0.01 vs. sham; &P < 0.01 vs. MI3D.

Immunofluorescence

We performed SCG10 immunofluorescence staining in the SCG (**Figure 2**). We observed that SCG10 in the sham group mainly gathered around the nucleus, while the cytoplasm rarely expressed. The MI1D group was similar to the sham group, and there was no significant change. However, from the third day of myocardial infarction, we found that the amount of SCG10 increased significantly, not only the number of positive cells, but also more expression in the cytoplasm, and there was a significant statistical significance compared with the sham group ($P < 0.01$). SCG10 positive cells of the MI7D group increased significantly compared with the MI3D group ($P < 0.01$), and the cytoplasm was full of positive fluorescence, indicating that SCG10 had been distributed throughout the cell of the neuron. The content of SCG10 in MI7D group was significantly lower than that in MI7D+SP600125 group in the SCG ($P < 0.01$) (**Figure 3**).

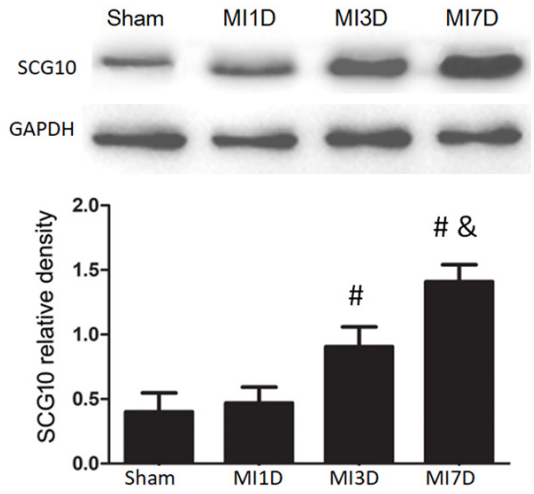

Figure 4. Western blot showing the expression profiles of SCG10 from the infracted border. SCG10 was quantified relative to the GAPDH (37 KD) levels. #P < 0.01 vs. sham; &P < 0.01 vs. MI3D.

Then we studied the difference of TH content around myocardial infarction border in rats (**Figure 4**). The expression of TH was very rare in the sham group. In the MI1D group the expression around the infarct area was also rare. There was no significant difference between the MI3D group and the sham group ($P > 0.05$). However, the expression of TH in MI7D group was significantly higher than that in the sham group ($P < 0.01$). The content of TH in MI7D group was significantly lower than that in MI7D+SP600125 group ($P < 0.01$) (**Figure 5**).

SCG10 protein expression in SCG and myocardium

In order to confirm the expression of SCG10 in the superior cervical ganglion and myocardium of rats after MI, we used the western blot method (**Figures 6**-**9**). It was found that the content

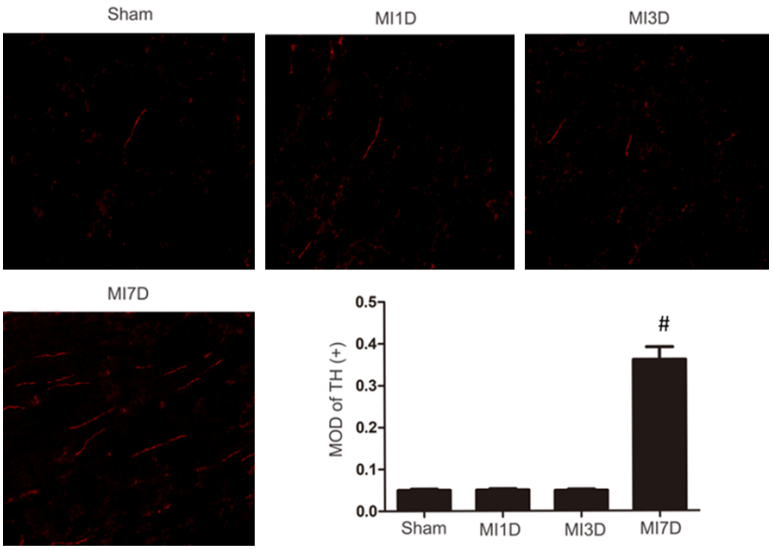

Figure 5. The immunofluorescence of tyrosine hydroxylase (TH) positive nerve fibers from the infracted border. #P < 0.01 vs. sham.

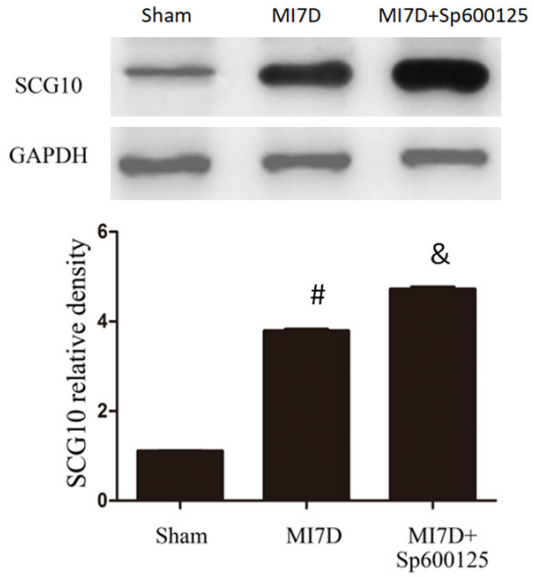

Figure 6. Western blot showing the expression profiles of SCG10 in the SCG after MI. SCG10 was quantified relative to the GAPDH (37 KD) levels. #P < 0.01 vs. sham; &P < 0.01 vs. MI7D.

of SCG10 in the SCG of the rats in MI1D group was not significantly different from that in the sham rats. However, the SCG10 level in the MI3D was significantly higher than that in the sham group ($P < 0.01$). MI7D group increased significantly compared with the MI3D group ($P < 0.01$). The content of SCG10 in MI7D group was significantly lower than that in MI7D+SP600125 group in the SCG ($P < 0.01$).

In the study of SCG10 content in rat myocardium, we found similar results. There was no significant difference between the MI1D group and the sham group, while the SCG10 level increased more significantly in MI3D group than the sham group ($P < 0.01$) and MI7D group increased significantly compared with the MI3D group ($P < 0.01$). The content of SCG10 in MI7D group was significantly lower than that in MI7D+SP600125 group in the myocardium ($P < 0.01$).

Discussion

After myocardial infarction, excessive regeneration of cardiac nerve, especially sympathetic nerve, is the main cause of increased mortality. At present, the mechanism of nerve regeneration is not clear [10, 11].

In normal axons, microtubules require transitions in polymerization and depolymerization to maintain the function of the axon, referred as "dynamic instability", which is vital to the survival of the normal axons [12, 13]. In mature axons, microtubules exist for hours or days, while in growing axons, the half-life of microtubules is only a few minutes. Taxol increases the stability of microtubule, which leads to the degeneration of the central neurites and causes neurological disease [14, 15]. Therefore, for newborn axons, excessive stability of microtubule cytoskeleton will be detrimental to the extension of axons [16, 17]. Cho's study found that the level of acetylated tubulin decreased significantly in the proximal stump of the injured nerve and increased the activity of microtubules, suggesting that microtubule instability is essential to axon regeneration [18].

Therefore, there must be some kind of protein and pathway to regulate the activity of microtubules in the neonatal axons [19, 20]. In the study of axonal dissection, the researchers found an interesting phenomenon that the fast consumption of SCG10 of the distal axons after transection of peripheral axons result in the degradation of distal axons, but the levels of

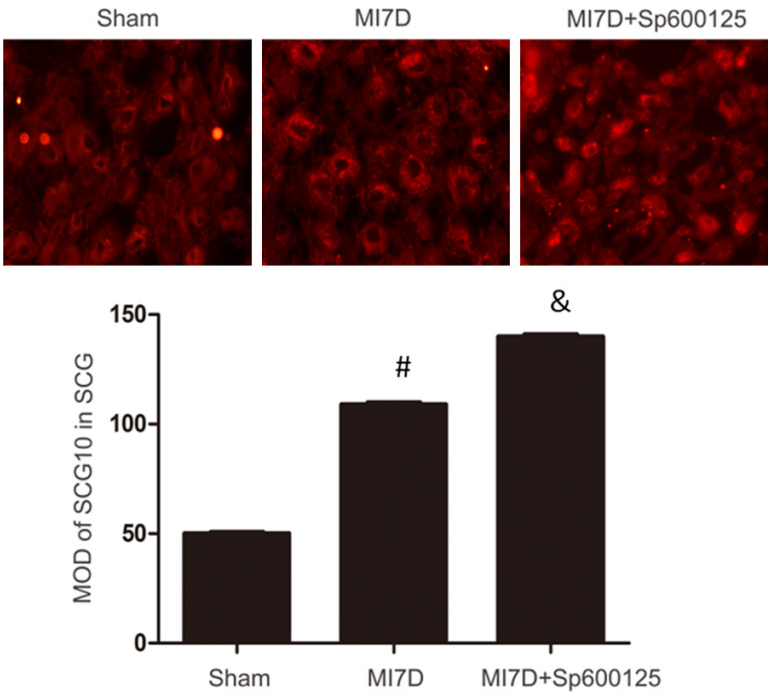

Figure 7. The immunofluorescence of SCG10 in SCG after myocardial infarction (MI). #P < 0.01 vs. sham; &P < 0.01 vs. MI7D.

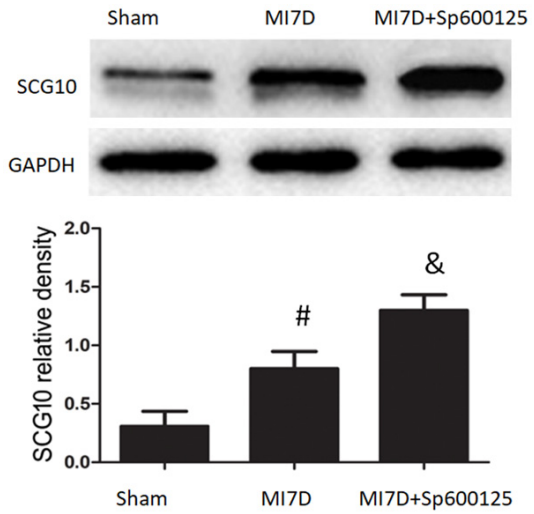

Figure 8. Western blot showing the expression profiles of SCG10 from the infracted border. SCG10 was quantified relative to the GAPDH (37 KD) levels. #P < 0.01 vs. sham; &P < 0.01 vs. MI7D.

SCG10 are increased in the end bulbs of the proximal stump. Our study also found a significant increase in SCG10 content in the peripheral axons of MI. Shin's study, which demonstrates that JNK can phosphorylate SCG10 in the distal axons of injured nerves, thus making SCG10 loss rapid in this segment [21, 22]. After preserving the SCG10 levels with JNK inhibitors, the degeneration of injured axons is significantly slowed down, which shows that SCG10 may play an important role in maintaining the stability for axon function. We injected JNK inhibitor on the basis of MI in rats, and also observed that the content of SCG10 in peripheral nerve axons of MI rats was significantly higher than that of only MI rats. Other studies also demonstrate that SCG10 accumulation in the proximal stump may correlate closely with axon regeneration after transection and ischemic brain injury.

Some studies have found that SCG10 is transported to the growth cone in the form of vesicles after being synthesized in neurons [23, 24]. Then the protein binds tubulin dimer and limits the pool of building for microtubule assembly causing microtubule instability [25]. In the process of neurite outgrowth, it especially requires the SCG10 induced "dynamic instability", which promotes the growth of axons [26, 27]. In conclusion, our study found that the increase of SCG10 content in the nerve growth cone around infarcted myocardium was positively correlated with the expression of TH-positive nerves, which further confirmed that SCG10-induced microtubule instability is an important mechanism for nerve regeneration.

In our research, the content of SCG10 on the axonal growth cone of infarcted myocardium did increase significantly, but we do not know where SCG10 came from. Clinical research demonstrated that removal of the superior cervical ganglion (SCG) results in the disappearance of symptoms of angina pectoris and the increase of blood pressure and cardiac sympathetic activity [28]. In our research group's previous animal experiments, we found that some signaling systems in the SCG can manage sympathetic nerve activity via NE after MI.

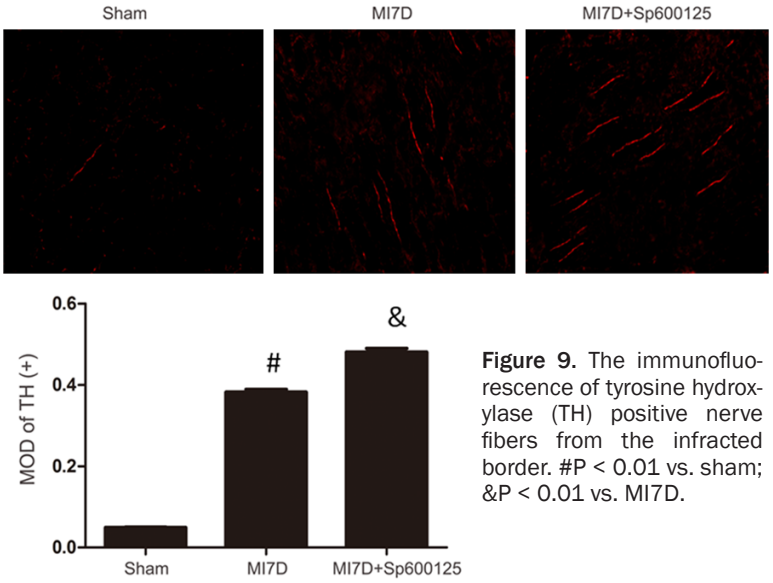

Figure 9. The immunofluorescence of tyrosine hydroxylase (TH) positive nerve fibers from the infracted border. #P < 0.01 vs. sham; &P < 0.01 vs. MI7D.

Therefore, we envisage that SCG is related to the changes of sympathetic activity and function after MI.

Our data show that the amount of SCG10 in the SCG has a significant increase with the progression of MI, and we have obtained consistent results by immunofluorescence and immunoblotting. When we injected JNK inhibitor into MI rats, the expression of SCG10 in SCG and myocardium was significantly higher than that in MI rats only. This indicates that the injury of the autonomic nervous system after MI leads to the massive synthesis of SCG10 in the SCG that transports through the axons to the nerve endings, thus participating in the injured nerve, especially the sympathetic nerve, and the repair and the maintenance of the function. However, we do not know the exact mechanism of SCG10 generation induced by nerve injury, which is the direction of further research.

When MI occurs, the cardiac sympathetic nerve releases a large amount of catecholamine, which is the main substance leading to malignant arrhythmia and further myocardial damage [29]. Tyrosine hydroxylase (TH) is a speed limiting enzyme for the synthesis of catecholamine and also plays a catalytic role [30]. Its positive location can represent the distribution of sympathetic nerves. In recent research, Parrish found that transient denervation of peri-infarct myocardium does not alter arrhymia susceptibility [31]. Therefore, reducing the remodeling of sympathetic nerves after MI is still the key to reduce the incidence of malignant arrhythmia. In our experiment, immunofluorescence showed that the density of TH-positive nerves around the infarcted area also changed with the content of SCG10 in nerve endings. The results showed that the decrease of SCG10 levels in nerve terminals ameliorated sympathetic hyperinnervation. The decrease of neurotransmitter released by sympathetic nerve will further reduce the incidence of malignant arrhythmia.

In conclusion, our data indicate that MI induced elevated levels of SCG10 in the SCG and infarcted border. The increase of SCG10 levels promotes axonal growth by the instability of tubulin and eventually resulted in hyperinnervation of sympathetic nerve in rats. This discovery may provide a new perspective for study of the mechanism of hyperinnervation and a potential therapeutic target for sympathetic remodeling and malignant arrhythmia after myocardial infarction.

Disclosure of conflict of interest

None.

Address correspondence to: Suhua Yan, Department of Cardiology, Shandong Qianfoshan Hospital, Cheeloo College of Medicine, Shandong University, No. 16766, Jingshi Road, Qingdao 266011, Shandong, China. Tel: +86-0531-89269418; E-mail: yansuhua116@yeah.net

References

[1] Liu X, Hou JL, Yang ZG, Xia CC, Xie LJ, Ye PF, Peng WL, Li L, Yang MX and Guo Y. Native T1 mapping for characterization of acute and chronic myocardial infarction in swine: comparison with contrast-enhanced MRI. J Magn Reson Imaging 2018; 47: 1406-1414.

[2] Nordlund D, Engblom H, Bonnet JL, Hansen HS, Atar D, Erlinge D, Ekelund U, Heiberg E, Carlsson M and Arheden H. Gender but not diabetes, hypertension or smoking affects infarct evolution in ST-elevation myocardial in-

farction patients - data from the CHILL-MI, MITOCARE and SOCCER trials. BMC Cardiovasc Disord 2019; 19: 161-166.
[3] Mauro AG, Bonaventura A, Mezzaroma E, Quader M and Toldo S. NLRP3 inflammasome in acute myocardial infarction. J Cardiovasc Pharmacol 2019; 74: 175-187.
[4] Green JL, Jacobs AK, Holmes D, Chiswell K, Blanco R, Bates ER, French W, Kupas DF, Mears G, Roe M and Nallamothu BK. Taking the reins on systems of care for ST-segment-elevation myocardial infarction patients: a report from the American Heart Association mission: lifeline program. Circ Cardiovasc Interv 2018; 11: 706.
[5] Díaz-Garzón J, Sandoval Y, Smith SW, Love S, Schulz K, Thordsen SE, Johnson BK, Driver B, Jacoby K, Carlson MD, Dodd KW, Moore J, Scott NL, Bruen CA, Hatch R and Apple FS. Discordance between ICD-coded myocardial infarction and diagnosis according to the universal definition of myocardial infarction. Clin Chem 2017; 63: 415-419.
[6] Fu CM, Chang CH, Lee CC, Fan PC, Chen SW, Lee CT, Wu CH, Li LC and Chen TH. Impact of dialysis dependence on prognosis in patients with myocardial infarction: an 11-year population-based study. Medicine (Baltimore) 2018; 97: 833-839.
[7] Peters SAE, Colantonio LD, Zhao H, Bittner V, Dai Y, Farkouh ME, Monda KL, Safford MM, Muntner P and Woodward M. Sex differences in high-intensity statin use following myocardial infarction in the united states. J Am Coll Cardiol 2018; 71: 1729-1737.
[8] Dolan EB, Hofmann B, de Vaal MH, Bellavia G, Straino S, Kovarova L, Pravda M, Velebny V, Daro D, Braun N, Monahan DS and Levey RE. A bioresorbable biomaterial carrier and passive stabilization device to improve heart function post-myocardial infarction. Mater Sci Eng C Mater Biol Appl 2019; 103: 751-755.
[9] Mehta SJ, Asch DA, Troxel AB, Lim R, Lewey J, Wang W, Zhu J, Norton L, Marcus N and Volpp KG. Comparison of pharmacy claims and electronic pill bottles for measurement of medication adherence among myocardial infarction patients. Med Care 2019; 57: 9-14.
[10] Desch S, Zeymer U and Thiele H. PCI strategies in acute myocardial infarction with cardiogenic shock. N Engl J Med 2018; 378: 1361-1365.
[11] Kwong JC, Schwartz KL, Campitelli MA, Chung H, Crowcroft NS, Karnauchow T, Katz K, Ko DT, McGeer AJ, McNally D, Richardson DC, Rosella LC, Simor A, Smieja M, Zahariadis G and Gubbay JB. Acute myocardial infarction after laboratory-confirmed influenza infection. N Engl J Med 2018; 378: 345-353.
[12] Hjort M, Lindahl B, Baron T, Jernberg T, Tornvall P and Eggers KM. Prognosis in relation to high-sensitivity cardiac troponin T levels in patients with myocardial infarction and non-obstructive coronary arteries. Am Heart J 2018; 200: 60-66.
[13] Faubert C, Heckman G and McKelvie R. Management of non-ST-elevation myocardial infarction in elderly patients: time to consider frailty and quality of life. Can J Cardiol 2018; 34: 241-243.
[14] Rymer JA, Tempelhof MW, Clare RM, Pieper KS, Granger CB, Van de Werf F, Moliterno DJ, Harrington RA, White HD, Armstrong PW, Lopes RD, Mahaffey KW and Newby LK. Discharge timing and outcomes after uncomplicated non-ST-segment elevation acute myocardial infarction. Am Heart J 2018; 201: 103-110.
[15] Vaccarino V, Sullivan S, Hammadah M, Wilmot K, Al Mheid I, Ramadan R, Elon L, Pimple PM, Garcia EV, Nye J, Shah AJ, Alkhoder A, Levantsevych O, Gay H, Obideen M, Huang M, Lewis TT, Bremner JD, Quyyumi AA and Raggi P. Mental stress-induced-myocardial ischemia in young patients with recent myocardial infarction: sex differences and mechanisms. Circulation 2018; 137: 794-805.
[16] Thackeray JT, Hupe HC, Wang Y, Bankstahl JP, Berding G, Ross TL, Bauersachs J, Wollert KC and Bengel FM. Myocardial inflammation predicts remodeling and neuroinflammation after myocardial infarction. J Am Coll Cardiol 2018; 71: 263-275.
[17] Dhar I, Lysne V, Seifert R, Svingen GFT, Ueland PM and Nygård OK. Plasma methionine and risk of acute myocardial infarction: effect modification by established risk factors. Atherosclerosis 2018; 272: 175-181.
[18] Wen LY, Yang ZG, Li ZL, Ai H, Xia CC, Zhang LZ, Lin BB, Zhang K, Fu H, Wu CQ, Yang L, Fan HM and Guo YK. Accurate identification of myocardial viability after myocardial infarction with novel manganese chelate-based MR imaging. NMR Biomed 2019; 32: e4158.
[19] Takahashi M. Cell-specific roles of NLRP3 inflammasome in myocardial infarction. J Cardiovasc Pharmacol 2019; 74: 188-193.
[20] Valley TS, Iwashyna TJ, Cooke CR, Sinha SS, Ryan AM, Yeh RW and Nallamothu BK. Intensive care use and mortality among patients with ST elevation myocardial infarction: retrospective cohort study. BMJ 2019; 365: 1927-1929.
[21] Krishnaswami A, Maurer MS and Alexander KP. Contextualizing myocardial infarction: comorbidities and priorities in older adults. Am J Med 2017; 130: 1144-1147.
[22] Zeitouni M, Silvain J, Guedeney P, Kerneis M, Yan Y, Overtchouk P, Barthelemy O, Hauguel-Moreau M, Choussat R, Helft G, Le Feuvre C, Collet JP and Montalescot G; ACTION Study Group. Periprocedural myocardial infarction

and injury in elective coronary stenting. Eur Heart J 2018; 39: 1100-1109.
[23] Marcolino MS, Maia LM, Oliveira JAQ, Melo LDR, Pereira BLD, Andrade-Junior DF, Boersma E and Ribeiro AL. Impact of telemedicine interventions on mortality in patients with acute myocardial infarction: a systematic review and meta-analysis. Heart 2019; 105: 1479-1486.
[24] Rozenbaum Z, Ravid D, Margolis G, Khoury S, Kaufman N, Keren G, Milwidsky A and Shacham Y. Association of pre-admission statin therapy and the inflammatory response in ST elevation myocardial infarction patients. Biomarkers 2019; 24: 17-22.
[25] Rodriguez-Granillo GA, Rodriguez AE and Milei J. Letter by Rodriguez-Granillo et al regarding article, "acute myocardial infarction: changes in patient characteristics, management, and 6-month outcomes over a period of 20 years in the FAST-MI program (French registry of acute ST-elevation or non-ST-elevation myocardial infarction) 1995 to 2015". Circulation 2018; 137: 2305-2306.
[26] Nordenskjöld AM, Baron T, Eggers KM, Jernberg T and Lindahl B. Predictors of adverse outcome in patients with myocardial infarction with non-obstructive coronary artery (MINOCA) disease. Int J Cardiol 2018; 261: 18-23.
[27] Ricottini E, Mangiacapra F, Nusca A, Melfi R, Cavallari I, Miglionico M, Gallo P, Pozzilli P and Di Sciascio G. Relation of platelet indexes to platelet reactivity and periprocedural myocardial infarction in patients who underwent percutaneous coronary angioplasty. Am J Cardiol 2018; 121: 1027-1031.
[28] Greenslade J, Cho E, Van Hise C, Hawkins T, Parsonage W, Ungerer J, Tate J, Pretorius C, Than M and Cullen L. Evaluating rapid rule-out of acute myocardial infarction using a high-sensitivity cardiac troponin i assay at presentation. Clin Chem 2018; 64: 820-829.
[29] Ćatić J, Jurin I, Lucijanić M, Jerkić H and Blaženković R. High red cell distribution width at the time of ST segment elevation myocardial infarction is better at predicting diastolic than systolic left ventricular dysfunction: a single-center prospective cohort study. Medicine (Baltimore) 2018; 97: 601-606.
[30] Cappelletti P, Morandini M, Moretti M, Malloggi L and Stenner E. How well do laboratories adhere to recommended clinical guidelines for the management of myocardial infarction? Clin Chem 2017; 63: 610-612.
[31] Shah M, Patnaik S, Maludum O, Patel B, Tripathi B, Agarwal M, Garg L, Agrawal S, Jorde UP and Martinez MW. Mortality in sepsis: comparison of outcomes between patients with demand ischemia, acute myocardial infarction, and neither demand ischemia nor acute myocardial infarction. Clin Cardiol 2018; 41: 936-944.